

# Thirst driving and suppressing signals encoded by distinct neural populations in the brain

Yuki Oka<sup>1,2,†</sup>, Mingyu Ye<sup>1,2</sup> & Charles S. Zuker<sup>1,2</sup>

Thirst is the basic instinct to drink water. Previously, it was shown that neurons in several circumventricular organs of the hypothalamus are activated by thirst-inducing conditions<sup>1</sup>. Here we identify two distinct, genetically separable neural populations in the subfornical organ that trigger or suppress thirst. We show that optogenetic activation of subfornical organ excitatory neurons, marked by the expression of the transcription factor ETV-1, evokes intense drinking behaviour, and does so even in fully water-satiated animals. The light-induced response is highly specific for water, immediate and strictly locked to the laser stimulus. In contrast, activation of a second population of subfornical organ neurons, marked by expression of the vesicular GABA transporter VGAT, drastically suppresses drinking,

even in water-craving thirsty animals. These results reveal an innate brain circuit that can turn an animal's water-drinking behaviour on and off, and probably functions as a centre for thirst control in the mammalian brain.

Body fluid homeostasis regulates the internal salt and water balance; as this balance shifts, the brain senses these changes and triggers specific goal-oriented intake behaviours<sup>2,3</sup>. For instance, salt-deprived animals may actively consume salty solutions, even though such high levels of salt are normally strongly aversive<sup>4–6</sup>. Similarly, dehydrated animals are strongly motivated to consume water<sup>7,8</sup>. Previous studies have shown that various regions in the circumventricular organs (CVO) of the hypothalamus are activated in response to dehydration<sup>1</sup>. In addition,

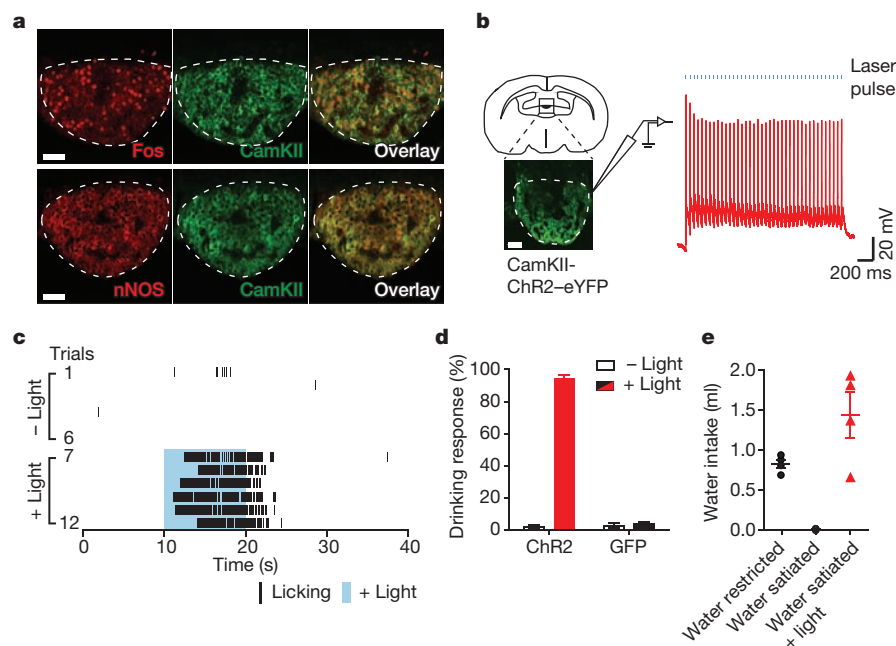


**Figure 1 | Activation of excitatory neurons in the SFO triggers immediate drinking behaviour.** **a**, Water-deprivation activates CamKII/nNOS-positive neurons in the SFO. Robust Fos expression was induced in the SFO after water restriction for 48 h. Shown are double immunolabelling for Fos and CamKII. Most Fos-positive neurons co-expressed CamKII ( $95.9 \pm 0.3\%$ ,  $n = 3$ ); also shown is the co-expression of CamKII with nNOS. These neurons are excitatory as they are marked by a VGlut2 transgenic reporter<sup>24</sup> (Extended Data Fig. 2). **b**, Whole-cell patch-clamp recording from SFO CamKII-positive neurons in acute hypothalamic slices demonstrating light-induced activation of the ChR2-expressing neurons. Shown are traces of a representative neuron subjected to 40 pulses of ChR2 excitation (20 Hz; 2 ms pulses); blue bars denote the time and duration of the light stimulus. Scale bars, 50  $\mu$ m. **c**, Photostimulation of CamKII-positive neurons in the SFO (trials 7–12; blue shading) triggered intense drinking; each black bar indicates an individual licking event. In the absence of light stimulation the same water-satiated animal

exhibits very sparse events of drinking (trials 1–6). **d**, Success of inducing drinking by photostimulation of the SFO. The drinking response (%) was calculated by determining the number of trials with more than five licks over the total number of trials; animals were tested for more than ten trials each (see Methods for details). The panel shows animals infected with AAV-CamKIIa-ChR2-eYFP ( $n = 10$ ; red bar), and control mice infected with AAV-CamKIIa-GFP (green fluorescent protein) ( $n = 4$ ; black bar); white bars indicate the responses in the absence of photostimulation (Mann–Whitney  $U$ -test  $P < 0.0003$ ). **e**, Quantitation of the volume of water consumed within 15 min by three groups of animals: water-restricted for 48 h, water-satiated, and water-satiated but photostimulated during the test; light (20 Hz) was delivered with a regime of 30 s on and 30 s off for the entire 15 min session ( $n = 4$ , Mann–Whitney  $U$ -test,  $P < 0.03$  for water-satiated  $\pm$  light). Values are means  $\pm$  s.e.m.

<sup>1</sup>Department of Biochemistry and Molecular Biophysics, Columbia College of Physicians and Surgeons, Howard Hughes Medical Institute, Columbia University, New York, New York 10032, USA.

<sup>2</sup>Department of Neuroscience, Columbia College of Physicians and Surgeons, Howard Hughes Medical Institute, Columbia University, New York, New York 10032, USA. <sup>†</sup>Present address: Division of Biology and Biological Engineering 216-76, California Institute of Technology, Pasadena, California 91125, USA.

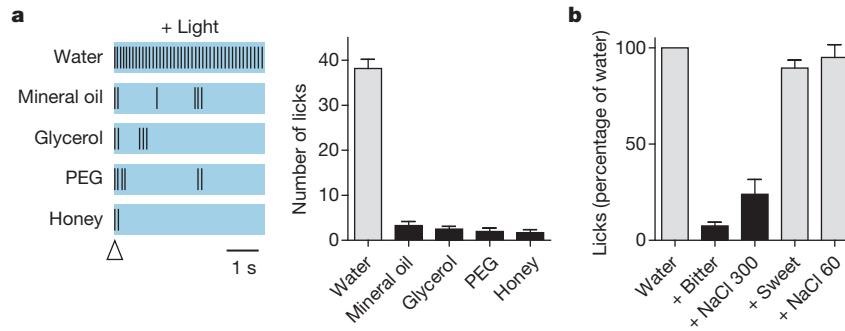


**Figure 2 | CamKII-positive SFO neurons mediate thirst.** Activation of CamKII-positive neurons in the SFO drives selective drinking of water. **a**, Representative raster plots illustrating licking events during a 5 s window in the presence of photostimulation; the open arrowhead indicates the first lick in each trial. The right panel shows quantification of similar data for multiple animals ( $n = 6$  for honey, and 7 for others; Mann–Whitney  $P < 0.002$ ); all

intracranial injection of angiotensin, a vasoactive hormone that stimulates drinking, has been shown to activate CVO neurons in several species<sup>9–11</sup>, and electrical stimulation of CVO nuclei increased fluid consumption in rodents<sup>12,13</sup>.

The subfornical organ (SFO) is one of several CVO nuclei activated by thirst-inducing stimuli (for example, water-deprivation)<sup>1,9</sup>. This nucleus lacks the normal blood–brain barrier, and has been proposed to function as an osmolality sensor in the brain<sup>1,14,15</sup>. We reasoned that if we could identify a selective population of neurons in the SFO that respond to dehydration, they might provide a genetic handle to explore the neural control of thirst and water-drinking behaviour. Using Fos as a marker for neuronal activation, we found that approximately 30% of the SFO neurons were strongly labelled with Fos after a 48-h water restriction regime (no Fos expression was observed under water-satiated conditions; Extended Data Fig. 1). Notably, essentially all of the Fos-labelled cells co-expressed Ca<sup>2+</sup>/calmodulin-dependent kinase II (CamKII; Fig. 1a upper panel), a known marker of excitatory neurons (see Extended Data Fig. 2), as well as neuronal nitric oxide synthase (nNOS; Fig. 1a lower panel). If these SFO neurons function as key cellular switches in the circuit that drives water consumption, then their activation should trigger water-drinking responses.

To test this hypothesis directly, we used an optogenetic approach<sup>16,17</sup>. We introduced ChR2 into the SFO by stereotaxic injection of an AAV-ChR2–eYFP (enhanced yellow fluorescent protein) construct under the control of the *CamkIIa*-promoter (Extended Data Fig. 3), and examined the effect of photostimulation in awake behaving animals (Figs 1b–e). Remarkably, photoactivation of the SFO CamKII-positive neurons *in vivo* triggered immediate water seeking behaviour followed by intensive drinking (Supplementary Video 1 and Fig. 1c). This response was tightly time-locked to the onset of laser stimulation, seen as long as the light stimulus was present, and could be reliably induced in over 90% of the trials (Fig. 1d). Upon termination of photostimulation the behaviour quickly ceased within a few seconds; light activation of the SFO in the absence of water had no effect on future drinking responses, even if the water was delivered just seconds after the light was switched off (Extended Data Fig. 4). Importantly, the light-induced drive to consume water was independent of the internal state of the animal as it was reliably evoked in fully water-satiated mice (Supplementary Video 2). Indeed, during a prolonged regime of laser stimulation, water-satiated mice continue to consume water avidly, and may drink nearly 8% of their body weight within 15 min; this is similar to the water consumption seen in the unstimulated animals after water restriction for 48 h (Fig. 1e). We note that light stimulation of the SFO did not induce feeding (Supplementary Video 3).

Next, we asked whether the light-induced ‘thirst’ is selective for water. Therefore, we assessed light-dependent fluid intake using a range of test solutions. Our results (Fig. 2a) show that the effect is highly specific for

animals were water-satiated. **b**, Photostimulated animals did not drink water in the presence of a bitter compound (3  $\mu$ M cycloheximide; paired *t*-test,  $P < 0.0001$ ), or high concentration of salt (300 mM; paired *t*-test,  $P < 0.001$ ), but did so in the presence of a sweet compound (30 mM sucrose), or low salt (60 mM); data were normalized to the number of licks to water alone. Values are means  $\pm$  s.e.m. ( $n = 5$  animals).

water, with no responses to other fluids such as mineral oil, glycerol, polyethylene glycol (PEG) or even honey. Notably, light-stimulated animals refused to drink water if it contained either a bitter compound or high concentrations of salt, demonstrating that photoactivation of these SFO neurons does not bypass the natural taste-mediated functions that prevent ingestion of toxic, noxious chemicals<sup>6</sup> (Fig. 2b).

We identified three genetically separable, non-overlapping populations in the SFO (Fig. 3a, b and Extended Data Fig. 5): an excitatory one

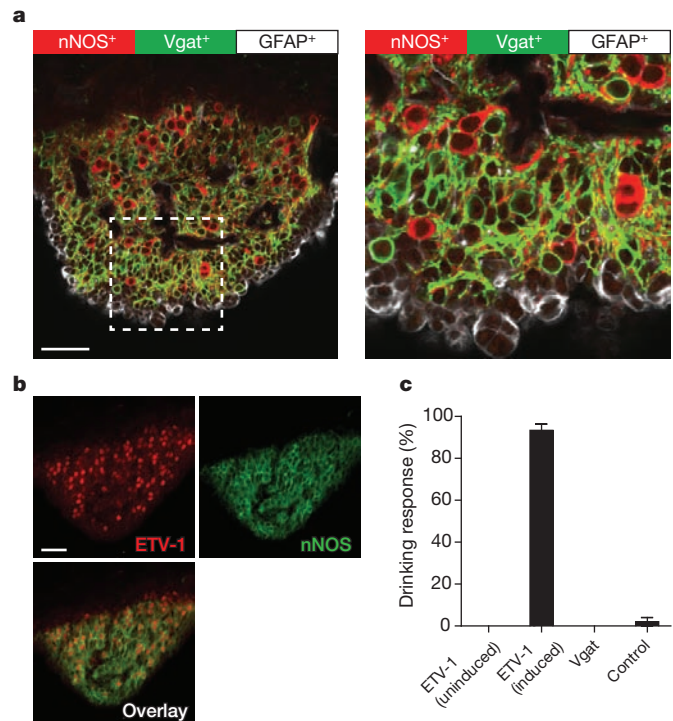


**Figure 3 | Three distinct cell populations in the SFO.** **a**, Tissue staining of the SFO from a transgenic animal expressing ChR2–eYFP in Vgat neurons (labelled with anti-GFP antibody, green) and co-labelled with anti-nNOS (red) and anti-GFAP antibodies (white); the right panel shows a magnified view illustrating the non-overlap between the three populations. **b**, ETV-1 (red) and nNOS (green) are co-expressed in most of the same neurons (>90% overlap,  $n = 3$ ). Scale bars, 50  $\mu$ m. **c**, Photostimulation of ChR2 in ETV-1-positive neurons triggers robust drinking responses in tamoxifen-induced ( $n = 6$ ), but not uninduced animals ( $n = 4$ ). In contrast, stimulation of ChR2 in Vgat ( $n = 8$ ) neurons or GFAP<sup>+</sup> glial cells (data not shown) had no effect on drinking behaviour. Control wild-type mice infected with AAV-flex-ChR2–eYFP showed no responses to light stimulation ( $n = 5$ ). Values are means  $\pm$  s.e.m.

defined by expression of CamKII/nNOS (see Extended Data Fig. 2), and overlapping with expression of the transcription factor ETV-1, a second one defined by the expression of the vesicular GABA transporter (Vgat), and a third expressing the glial fibrillary acidic protein (GFAP; Fig. 3a). As expected, optogenetic stimulation of the ETV-1-positive neurons mimicked the effect of activating the CamKII-positive neurons and robustly triggered drinking behaviour in water-satiated animals (Fig. 3c). The *Etv1-Cre* mouse line<sup>18</sup> used in these experiments was tamoxifen inducible<sup>19</sup> (Cre-ER), and correspondingly, the behaviour was fully dependent on tamoxifen induction. Photostimulation of the other two populations did not stimulate drinking (Fig. 3c and data not shown).

Given that the CamKII/ETV-1-positive neurons provide a 'thirst-on' signal, we wondered whether one of the other cell classes might encode a 'thirst-off' signal. Indeed, activation of the Vgat-positive neurons significantly suppressed water intake in thirsty animals (>80% lick suppression); the effect was time-locked to the laser stimulation, and observed in all Vgat ChR2-expressing animals tested (Fig. 4a, b). Significantly, the suppression was as effective in thirsty animals that were actively drinking water, as it was in thirsty animals that had not yet sampled water (compare Fig. 4a, c).

If activation of Vgat-positive neurons 'quenches' thirst, then the effect should be highly specific for the motivation or drive to drink water. Thus, we examined the effect of photostimulation on salt appetite in salt-craving animals, and in sugar-intake in hungry animals (Fig. 4d, e; see also Methods). As hypothesized, activation of Vgat-positive neurons specifically extinguished the craving to consume water, but did not affect food or salt appetite. Taken together, these results substantiate Vgat-positive neurons as mediators of the 'thirst-off' signal, and demonstrate that the SFO contains selective populations of neurons mediating physiologically opposite responses to thirst.

Thirst is a fundamental physiological state representing a basic and innate response to dehydration. Earlier studies using micro-electrical

stimulation and hormonal injections implicated the SFO in fluid homeostasis<sup>9,12,13</sup>, and possibly salt appetite<sup>20,21</sup>. Here we have shown that the craving for water can be controlled with cell-type-specific precision in the SFO.

We used a combination of genetic and optogenetic tools in awake, behaving animals to demonstrate that the ETV-1- and Vgat-positive neurons of the SFO evoke or suppress the motivation to drink, respectively. We have shown that activation of either population instantly triggers the behaviour, be it water-seeking and drinking in normal or water-satiated animals, or strong suppression of drinking in thirsty animals; these responses are selective to water-drinking, with no effect on feeding or salt appetite. Significantly, most of the neurons in the SFO are either ETV-1-positive or Vgat-positive (Fig. 3), strongly arguing that the SFO is a dedicated brain system for thirst, functioning possibly at the interface between the physiological/internal state of the organism and the motivation to drink water. Interestingly, the ETV-1 neuronal population selectively expresses the angiotensin receptor AT1 (Extended Data Fig. 6), identifying these neurons as a possible target of angiotensin-mediated drinking responses<sup>9–11</sup>.

In addition to the SFO, dehydration activates several other brain regions<sup>8,15</sup>, including the organum vasculosum of the lamina terminalis<sup>1</sup>, another hypothalamic nucleus lacking the blood–brain barrier. Notably, this nucleus has direct connections to the SFO<sup>22,23</sup>. Indeed, as an entry to dissect the circuit for thirst further, we surveyed the axonal projections from the ETV-1 and Vgat-expressing neurons in the SFO. Our results (Extended Data Fig. 7) show that both classes of SFO neurons project to the organum vasculosum of the lamina terminalis and the median preoptic nucleus. Interestingly, the glutamatergic neurons (that is, excitatory), unlike the GABAergic neurons, also project to the supraoptic nucleus and the paraventricular hypothalamic nucleus. Future physiological and behavioural studies should help reveal the role of these nodes in the neural circuitry mediating thirst, and their association with brain centres involved in other motivational states.

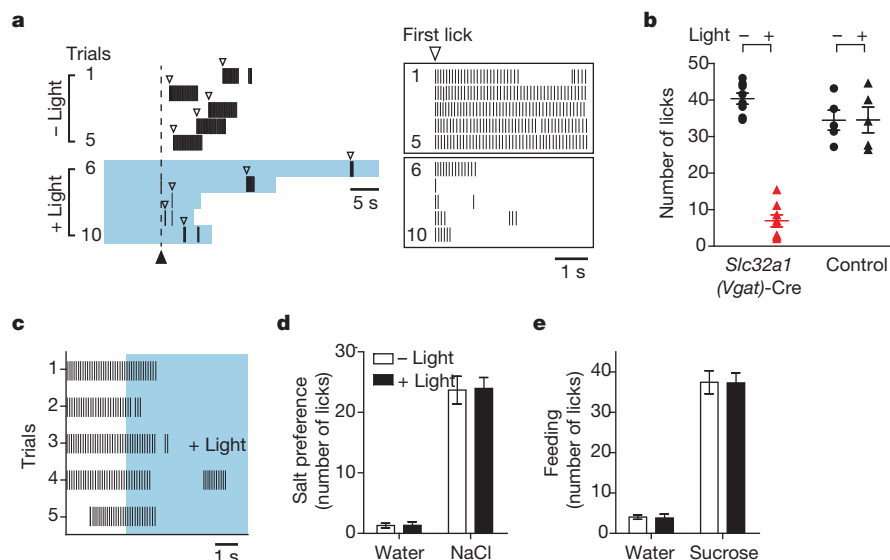


**Figure 4 | Activation of Vgat-positive neurons in the SFO suppresses thirst.**

**a**, Drinking behaviour of a 24-h water-deprived animal expressing ChR2 in Vgat-positive neurons. Trials were performed in the absence (trials 1–5) or presence of photostimulation (trials 6–10). The filled arrowhead indicates the time of water presentation, and the open arrowheads mark the first lick; animals were allowed to lick for 5 s following the first lick in each trial. Light stimulation (blue shading) was started 10 s before water presentation, and maintained until the end of the 5 s licking window. The boxes on the right show an enlargement of these ten trials, each aligned to the first lick. Note the strong suppression during photostimulation. **b**, Graph quantifying the degree of suppression in animals expressing AAV-flex-ChR2-eYFP in Vgat-positive neurons of the SFO (*Slc32a1-Cre*<sup>24</sup>) with or without light stimulation

(Mann–Whitney *U*-test,  $P < 0.002$ ;  $n = 8$ ). Also shown are wild-type control mice infected with the same AAV-flex-ChR2-eYFP construct ( $n = 5$ ). Animals were tested for more than five trials each, and the total number of licks was averaged across trials. Photostimulation of the GFAP-positive population had no effect on drinking (data not shown). **c**, Activation of Vgat-positive neurons suppresses drinking behaviour even if animals were actively drinking. The plot illustrates the drinking response of a thirsty animal in five tests, before and during photostimulation (blue shading); the trials were aligned 3 s before photostimulation. **d, e**, Photostimulation of Vgat-positive neurons did not suppress salt appetite in salt-depleted animals (150 mM NaCl), or sugar intake in hungry animals (300 mM sucrose); values are means  $\pm$  s.e.m. ( $n = 7$ ).

**Online Content** Methods, along with any additional Extended Data display items and Source Data, are available in the online version of the paper; references unique to these sections appear only in the online paper.

**Received 2 September; accepted 24 November 2014.**

**Published online 26 January 2015.**

- McKinley, M. J. *et al.* The sensory circumventricular organs of the mammalian brain. *Adv. Anat. Embryol. Cell Biol.* **172**, 1–122 (2003).
- Young, J. K. *Hunger, Thirst, Sex, and Sleep: How the Brain Controls Our Passions* (Rowman & Littlefield, 2012).
- Sternson, S. M. Hypothalamic survival circuits: blueprints for purposive behaviors. *Neuron* **77**, 810–824 (2013).
- Daniels, D. & Fluharty, S. J. Salt appetite: a neurohormonal viewpoint. *Physiol. Behav.* **81**, 319–337 (2004).
- Geerling, J. C. & Loewy, A. D. Central regulation of sodium appetite. *Exp. Physiol.* **93**, 177–209 (2008).
- Oka, Y., Butnaru, M., von Buchholtz, L., Ryba, N. J. & Zuker, C. S. High salt recruits aversive taste pathways. *Nature* **494**, 472–475 (2013).
- Stricker, E. M. & Sved, A. F. Thirst. *Nutrition* **16**, 821–826 (2000).
- McKinley, M. J. & Johnson, A. K. The physiological regulation of thirst and fluid intake. *News Physiol. Sci.* **19**, 1–6 (2004).
- Fitzsimons, J. T. Angiotensin, thirst, and sodium appetite. *Physiol. Rev.* **78**, 583–686 (1998).
- Epstein, A. N., Fitzsimons, J. T. & Simons, B. J. Drinking caused by the intracranial injection of angiotensin into the rat. *J. Physiol. (Lond.)* **200**, 98–100 (1969).
- Sturgeon, R. D., Brophy, P. D. & Levitt, R. A. Drinking elicited by intracranial microinjection of angiotensin in the cat. *Pharmacol. Biochem. Behav.* **1**, 353–355 (1973).
- Robertson, A., Kucharczyk, J. & Mogenson, G. J. Drinking behavior following electrical stimulation of the subfornical organ in the rat. *Brain Res.* **274**, 197–200 (1983).
- Smith, P. M., Beninger, R. J. & Ferguson, A. V. Subfornical organ stimulation elicits drinking. *Brain Res. Bull.* **38**, 209–213 (1995).
- Verbalis, J. G. How does the brain sense osmolality? *J. Am. Soc. Nephrol.* **18**, 3056–3059 (2007).
- Bourque, C. W., Oliet, S. H. & Richard, D. Osmoreceptors, osmoreception, and osmoregulation. *Front. Neuroendocrinol.* **15**, 231–274 (1994).
- Li, X. *et al.* Fast noninvasive activation and inhibition of neural and network activity by vertebrate rhodopsin and green algae channelrhodopsin. *Proc. Natl Acad. Sci. USA* **102**, 17816–17821 (2005).
- Boyden, E. S., Zhang, F., Bamberg, E., Nagel, G. & Deisseroth, K. Millisecond-timescale, genetically targeted optical control of neural activity. *Nature Neurosci.* **8**, 1263–1268 (2005).
- Taniguchi, H. *et al.* A resource of Cre driver lines for genetic targeting of GABAergic neurons in cerebral cortex. *Neuron* **71**, 995–1013 (2011).
- Feil, R. *et al.* Ligand-activated site-specific recombination in mice. *Proc. Natl Acad. Sci. USA* **93**, 10887–10890 (1996).
- Hiyama, T. Y., Watanabe, E., Okado, H. & Noda, M. The subfornical organ is the primary locus of sodium-level sensing by Na<sup>v</sup> sodium channels for the control of salt-intake behavior. *J. Neurosci.* **24**, 9276–9281 (2004).
- Noda, M. & Sakuta, H. Central regulation of body-fluid homeostasis. *Trends Neurosci.* **36**, 661–673 (2013).
- Johnson, A. K., Zardetto-Smith, A. M. & Edwards, G. L. Integrative mechanisms and the maintenance of cardiovascular and body fluid homeostasis: the central processing of sensory input derived from the circumventricular organs of the lamina terminalis. *Prog. Brain Res.* **91**, 381–393 (1992).
- Johnson, A. K. & Gross, P. M. Sensory circumventricular organs and brain homeostatic pathways. *FASEB J.* **7**, 678–686 (1993).
- Vong, L. *et al.* Leptin action on GABAergic neurons prevents obesity and reduces inhibitory tone to POMC neurons. *Neuron* **71**, 142–154. 10.1016/j.neuron.2011.05.028 (2011).

**Supplementary Information** is available in the online version of the paper.

**Acknowledgements** We thank N. Propp for help with mouse husbandry. We also thank H. Fishman for suggestions, Z. Turan, N. Ryba and T. Usdin for technical support, and N. Ryba and members of the Zuker laboratory for comments. We acknowledge B. Lowell and M. Krashes for advice. Y.O. and M.Y. were supported by grants from the National Institute on Drug Abuse and National Institute of Neurological Disorders and Stroke to C.S.Z. C.S.Z. is an investigator of the Howard Hughes Medical Institute.

**Author Contributions** Y.O. developed the research program, designed the study, carried out the experiments, and analysed data; M.Y. performed all slice patch clamp recordings; C.S.Z. analysed data, designed experiments and together with Y.O. wrote the paper.

**Author Information** Reprints and permissions information is available at [www.nature.com/reprints](http://www.nature.com/reprints). The authors declare no competing financial interests. Readers are welcome to comment on the online version of the paper. Correspondence and requests for materials should be addressed to Y.O. ([yoka@caltech.edu](mailto:yoka@caltech.edu)).



## METHODS

**Animals.** All procedures were in accordance with the US National Institutes of Health (NIH) guidelines for the care and use of laboratory animals, and were approved by the Columbia University Animal Care and Use Committee. Reported data were obtained from mice ranging from 1.5 to 4 months of age and from both genders; randomization and blinding methods were not used. C57BL/6J and transgenic animals were acquired from the Jackson Laboratory (*Etv1*-CreER; stock number 013048, *Gfap*-Cre; stock number 012886, *Slc32a1* (*Vgat*)-Cre; stock number 016962, Ai9; stock number 007909, and *Slc17a6* (*Vglut2*)-Cre; stock number 016963). The *Etv1*-CreER line was originally developed in ref. 18; *Gfap*-Cre line was originally developed in ref. 25; *Slc32a1/Slc17a6*-Cre lines were originally developed in ref. 24, Ai9 (Rosa-flex-tdTomato<sup>26</sup>). Animals were housed in a temperature-controlled environment with a 12-h light and 12-h dark cycle. Mice had *ad libitum* access to food and water except during behavioural tests. Sample sizes were chosen to allow robust statistical analysis of data; no statistical method was used to determine sample size. Representative data were chosen on the basis of at least three independent experiments.

**Viral constructs.** AAV viruses were prepared by the University of Pennsylvania Vector Core (AAV9.EF1 $\alpha$ .DIO.ChR2-eYFP.WPRE,  $1.07 \times 10^{13}$  to  $1.6 \times 10^{13}$  genomic copies per millilitre; AAV9.CamKII $\alpha$ .ChR2-eYFP.WPRE,  $1.06 \times 10^{13}$  to  $1.98 \times 10^{13}$  genomic copies per millilitre; AAV9.CamKII $\alpha$ .GFP.WPRE,  $1.71 \times 10^{13}$  genomic copies per millilitre; AAV9.CB7Cl.mCherry.WPRE,  $9.22 \times 10^{12}$  genomic copies per millilitre; AAV9.CAG.flex.tdTomato.WPRE.bGH,  $8.88 \times 10^{12}$  genomic copies per millilitre).

**Surgery.** Adult 1.5- to 4-month-old mice were anaesthetized with ketamine and xylazine (100 mg per kg and 10 mg per kg, intraperitoneally) and placed under a stereotaxic apparatus (Narishige). During surgery, body temperature was monitored and controlled using a closed-loop heating system (FHC). Procedures for surgery and virus injection were similar to those described previously<sup>27–29</sup>. A small craniotomy with a diameter of less than 1 mm was performed at approximately bregma  $-0.55$  (anterior–posterior),  $0$  (medial–dorsal). AAV ( $<40$  nl total volume) was injected into the SFO by pressure injection (Nanoliter 2000, World Precision Instruments) using a pulled glass capillary at approximately  $10$  nl min<sup>-1</sup>. The coordinates for injection into the SFO were Bregma  $-0.55$  (anterior–posterior),  $0$  (medial–dorsal) and  $3.0$  (dorsal–ventral). After injection, a 200- $\mu$ m fibre bundle (ThorLabs) attached to a custom-modified ferrule (Precision Fiber Products) was placed less than 300  $\mu$ m dorsal to the injection site, and permanently fixed on the skull with dental cement (Lang Dental Manufacturing). Cannulated animals were allowed to recover for at least 8 days after surgery. In *Etv1*-CreER mice<sup>18</sup>, Cre-mediated ChR2 expression was induced by the injection of tamoxifen (80 mg per kg body weight for two or three times) after the recovery period. For tracing experiments, *Etv1*-CreER and *Slc32a1*-Cre mice were injected with AAV-flex-tdTomato-WPRE.bGH ( $<10$  nl total volume). To minimize the likelihood of ‘spill-over’ infection in *Slc32a1*-Cre mice, we diluted AAV by a factor of 10 before injection.

**Behavioural assays.** Brief water access test. Animals were tested in a custom gustometer as described previously<sup>6,30</sup>. Individual trials were either 40 s (stimulation of drinking) or 60 s (suppression of drinking) duration with a minimum intertrial interval of 40 s. Trials automatically terminated 5 s after the first lick, and the number of licks in this 5-s licking window was used to quantify responses. All experiments with 24-h water restriction were performed in their home cage before testing. For experiments that extended for 48-h, animals were provided with 1 ml of water after 24 h. For salt-attraction assays (Fig. 4d), mice were injected with furosemide<sup>6</sup> (50 mg per kg) and were kept for 24 h with salt-deficient food (Harlan). For feeding assays (Fig. 4e), animals were food-restricted for 24 h. Data were statistically analysed using Mann–Whitney *U*- or two-tailed paired *t*-tests. After behavioural assays, animals were perfused with 4% PFA and the SFO was examined to confirm viral expression. Animals that showed no detectable viral expression in the SFO were excluded from analysis.

ChR2-mediated stimulation of drinking. Laser pulses (473 nm, 20 ms) at 20 Hz were delivered through an optic fibre bundle using a laser pulse generator (Shanghai Laser & Optics Century). The laser output was maintained at 10 mW as measured at the tip of the fibre. In each 40-s trial, animals were photostimulated for up to 20 s (10–30 s window); stimulation was terminated when the trial ended. Photostimulation was triggered manually in each trial. Animals were tested for 3–20 trials for each condition, and the number of licks was averaged across trials. Because the spout shutter automatically closed 5 s after the first lick, we excluded trials where the animals made the first lick before the experiment (photostimulation) started (0–10 s window). To analyse the efficacy of photostimulation in inducing drinking responses (Figs 1d and 3c), we determined the number of trials with more than five licks over the total number of trials. In essence, animals were photostimulated for 20 s, and we measured the number of licks during the first 5-s after they reached the spout (these were freely moving animals). If the animals exhibited more than five licks within the 5-s window, the trial was considered positive (shown as drinking

response (%)). In Fig. 1c, animals were photostimulated for 10 s with water available for the full 40-s trial. In Fig. 1e, animals were placed in a gustometer and photostimulation was delivered with a regime of 30 s on and 30 s off for the entire 15 min session. We measured total amount of consumed water by weighing the water bottle before and after the session.

ChR2-mediated drinking suppression. Animals were subjected to water restriction (Fig. 4a–c), salt-deprivation (Fig. 4d) or food-deprivation (Fig. 4e) for 24 h before behavioural experiments. In each 60 s trial, 473 nm laser pulses (20 ms; 10 mW at fibre tip) at 20 Hz was started 10 s before water presentation, and maintained until the end of the trial. The number of licks in a 5 s window following the first lick was analysed. Animals were tested for three to ten trials each, and the number of licks was averaged across trials.

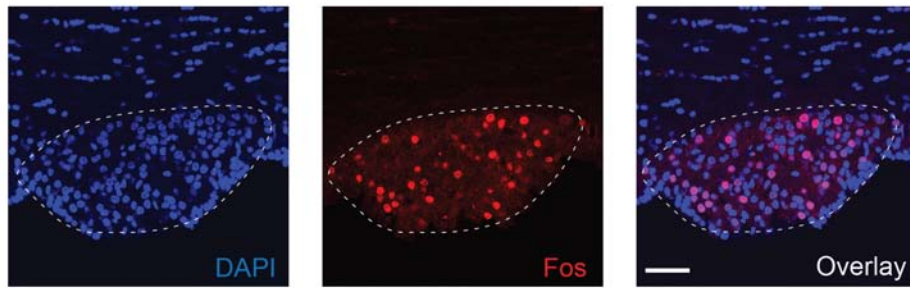
**Histology.** Animals were killed with ketamine and xylazine, and perfused with 10 ml of PBS followed by 10 ml of 4% PFA in PBS (pH 7.4). Brains were dissected and post-fixed overnight in 4% PFA in PBS. Coronal brain sections (100  $\mu$ m) were prepared using a vibratome (VT-1000S, Leica). After blocking with 10% FBS/0.2% Triton X-100 in PBS in the presence of 0.2% Triton X-100 for 1 h, sections were incubated with primary antibodies overnight at 4 °C. The primary antibodies (1:500 dilution) used in these studies were as follows: rabbit anti-CamKII (Abcam, ab5683), goat anti-c-Fos (Santa Cruz, SC-52G), goat anti-GFAP (Abcam, ab53554), rabbit anti-nNOS (Santa Cruz, sc-648), goat anti-nNOS (abcam ab72428), rabbit anti-ETV-1 (Abcam, ab81086) and chicken anti-GFP (Abcam, ab13970). Sections were washed twice with PBS, followed by incubation for more than 3 h with fluorophore-conjugated secondary antibodies (1:500 dilution, Jackson ImmunoResearch). Fluorescent images were acquired and processed using a confocal microscope (FV1000, Olympus). In some experiments, brain sections were counterstained with DAPI (Sigma Aldrich).

**Electrophysiological recordings from the SFO neurons in acute slice preparation.** Procedures for preparing acute brain slices and whole-cell recordings with optogenetic stimulations were similar to those described previously<sup>29</sup>. Coronal slices containing the SFO (250  $\mu$ m thick) were sectioned using a vibratome (VT-1000S, Leica) in ice-cold sucrose-based solution (in mM: 213 sucrose, 26 NaHCO<sub>3</sub>, 10 dextrose, 2.5 KCl, 2.0 MgSO<sub>4</sub>, 2.0 CaCl<sub>2</sub> and 1.23 NaH<sub>2</sub>PO<sub>4</sub>, aerated with 95% O<sub>2</sub>/5% CO<sub>2</sub>). Slices were transferred to oxygenated artificial cerebrospinal fluid (composition in mM: 126 NaCl, 26 NaHCO<sub>3</sub>, 2.5 KCl, 2 MgSO<sub>4</sub>, 2 CaCl<sub>2</sub>, 1.25 NaH<sub>2</sub>PO<sub>4</sub> and 25 dextrose, 315 mOsm, adjusted to pH 7.4) and incubated at 32 °C for at least 40 min. SFO neurons infected with AAV-CamKII-ChR2-eYFP *in vivo* were visualized by differential interference contrast. Whole-cell current clamp recordings were performed at 32 °C with an Axopatch 200B amplifier and a Digidata 1440A (Molecular Devices). The patch electrode (4–6 M $\Omega$ ) was filled with intracellular solution (in mM: 140 Kgluconate, 3 KCl, 2 MgCl<sub>2</sub>, 10 HEPES, 0.2 EGTA, and 2 Na<sub>2</sub>ATP, 290 mOsm, adjusted to pH 7.2). Data were filtered at 5 kHz, sampled at 20 kHz and analysed with pClamp10 software (Molecular Devices). Photostimulation was by means of an X-Cite XLED1 (Lumen Dynamics; 470 nm, 2 ms pulses at 20 Hz).

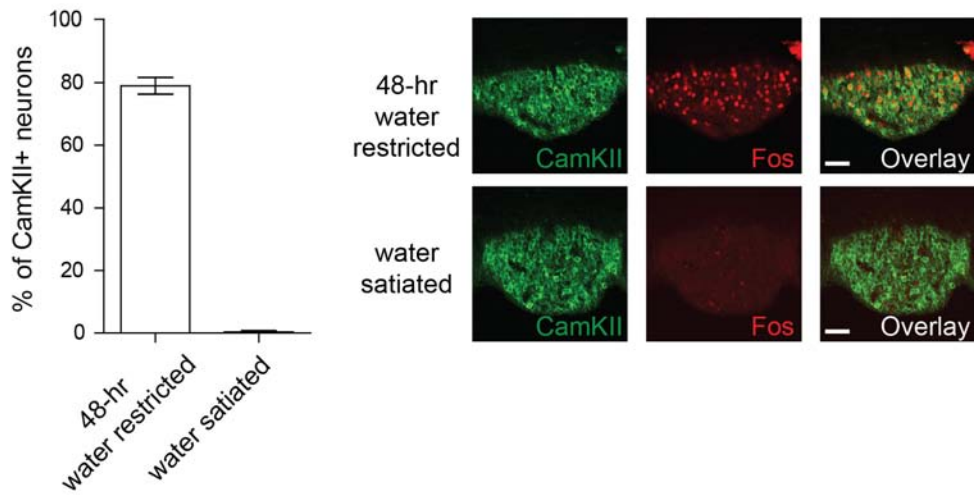
**Quantitative PCR.** The SFO from *Etv1*-CreER/Ai9 or *Slc32a1*-Cre/Ai9 mice were dissected under a fluorescence microscope, ensuring minimal addition of adjoining tissue. The SFO was dissociated into single cells using Papain Dissociation System (Worthington), labelled with DAPI and the tdTomato<sup>+</sup> neurons sorted using a flow cytometer (MoFlo Astrios, Beckman Coulter). RNA was extracted using a PicoPure RNA isolation kit (Applied Biosystems) and complementary DNA prepared using an Ovation RNA-seq V2 kit (Nugen). Quantitative real-time PCR used the following sets of primers: ETV-1 (5' primer: CAAACATCCCCCTCCACCA; 3' primer: ATAGAAGCTGGGACCCT), nNOS (5' primer: CGGGAATCAGGAGTTGCAGT; 3' primer: CAGAGCGGTGTTCCTTTCCT), *Vgat* (5' primer: TCATC GAGCTGGTGTGACG; 3' primer: CTTGGACACGGCCTTGAGAT), AT1 (5' primer: CACTGCCTGAACCCTCTGT; 3' primer: TCCACCTCAGAACAAGACGC), GAPDH (5' primer: GGTTGTCTCTGCGACTTCA; 3' primer: TAGG GCCTCTCTTGCTCAGT). Data were normalized to GAPDH.

25. Garcia, A. D., Doan, N. B., Imura, T., Bush, T. G. & Sofroniew, M. V. GFAP-expressing progenitors are the principal source of constitutive neurogenesis in adult mouse forebrain. *Nature Neurosci.* **7**, 1233–1241 (2004).
26. Madisen, L. et al. A robust and high-throughput Cre reporting and characterization system for the whole mouse brain. *Nature Neurosci.* **13**, 133–140 (2010).
27. Wu, Z., Autry, A. E., Bergan, J. F., Watabe-Uchida, M. & Dulac, C. G. Galanin neurons in the medial preoptic area govern parental behaviour. *Nature* **509**, 325–330 (2014).
28. Aponte, Y., Atasoy, D. & Sternson, S. M. AGRP neurons are sufficient to orchestrate feeding behavior rapidly and without training. *Nature Neurosci.* **14**, 351–355 (2011).
29. Lee, H. et al. Scalable control of mounting and attack by Esr1<sup>+</sup> neurons in the ventromedial hypothalamus. *Nature* **509**, 627–632 (2014).
30. Chandrashekar, J. et al. The cells and peripheral representation of sodium taste in mice. *Nature* **464**, 297–301 (2010).
31. Ng, L. et al. An anatomic gene expression atlas of the adult mouse brain. *Nature Neurosci.* **12**, 356–362 (2009).
32. Yoneshima, H. et al. Er81 is expressed in a subpopulation of layer 5 neurons in rodent and primate neocortices. *Neuroscience* **137**, 401–412 (2006).

a



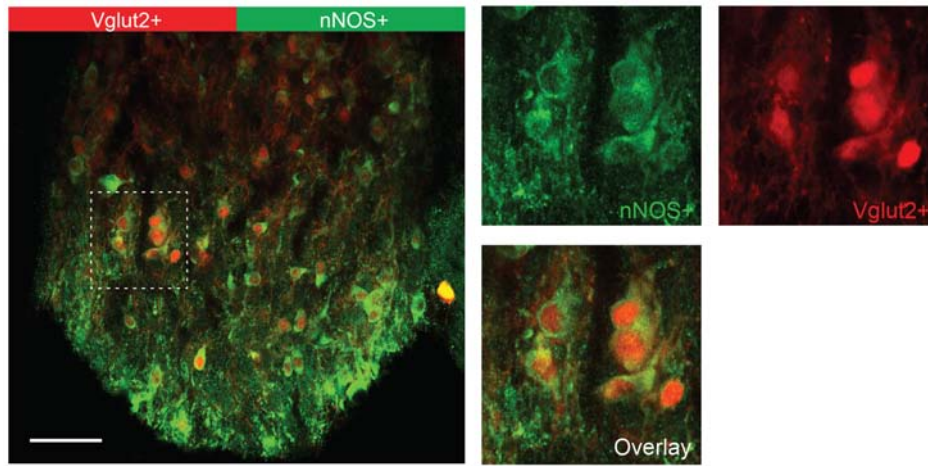
b



**Extended Data Figure 1 | Fos induction by water deprivation in the SFO.**

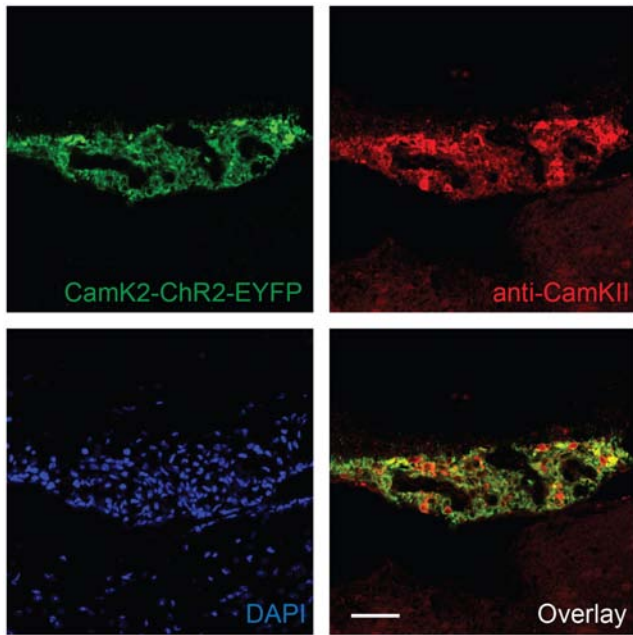
**a**, Approximately 30% of cells in the SFO (visualized with 4',6-diamidino-2-phenylindole (DAPI) staining, blue) of a water-restricted animal (48 h) are Fos-positive (red,  $26 \pm 1.9\%$ ,  $n = 3$ ). **b**, No significant Fos labelling was

detected under the water-satiated condition (lower panel). Scale bar, 50  $\mu\text{m}$ . The graph shows quantification of Fos-positive cells among CamKII<sup>+</sup> neurons, both under water-restricted and satiated conditions. Values are means  $\pm$  s.e.m. ( $n = 3$ ).



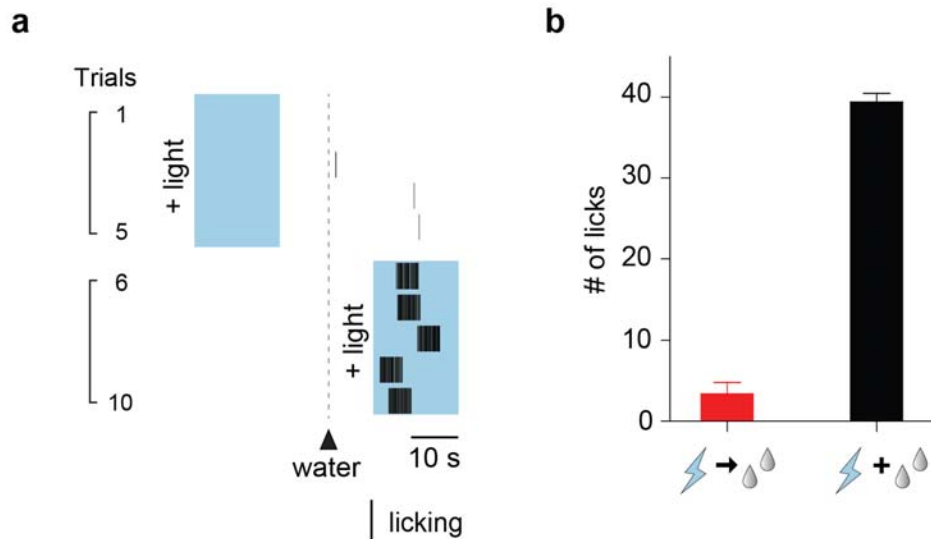
**Extended Data Figure 2 | nNOS-positive neurons in the SFO co-express Vglut2, an excitatory neuronal marker.** nNOS antibody staining (green) of the SFO from a *Slc17a6*-Cre/Ai9 transgenic animal expressing tdTomato in

Vglut2-positive neurons (red); the right panel shows a magnified view illustrating the overlap between tdTomato- and nNOS-positive signals. Scale bar, 50  $\mu$ m.



**Extended Data Figure 3 | Virally expressed ChR2-eYFP under the control of CamKII promoter co-localized with endogenous CamKII.** Tissue staining of the SFO in a wild-type animal infected with AAV-CamKIIa-ChR2-eYFP. Expression of ChR2-eYFP (labelled with anti-GFP antibody) overlapped endogenous CamKII expression (anti-CamKII antibody, upper right). Lower left panel shows DAPI staining (blue). Scale bar, 50  $\mu$ m.

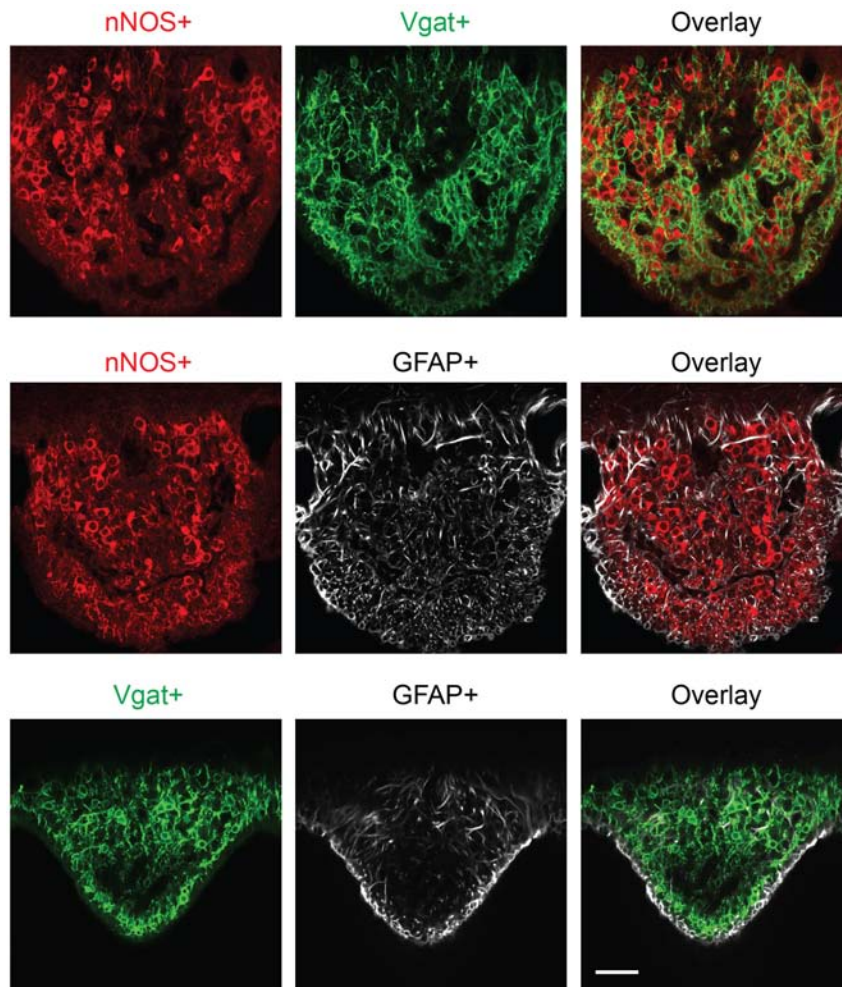




**Extended Data Figure 4 | ChR2-dependent drinking requires activation of SFO CamKII-positive neurons concurrently with water presentation.**

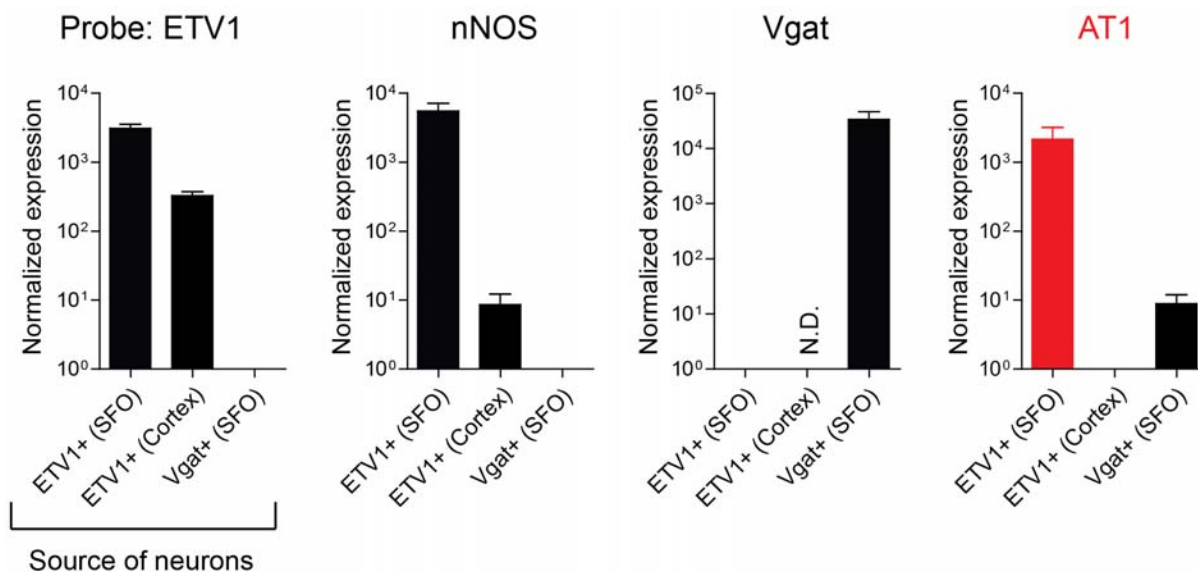
**a**, Representative raster plots illustrating drinking behaviour in a wild-type animal expressing ChR2-eYFP under the control of CamKII promoter. Trials were performed with photostimulation (blue shadings) delivered before (trials 1–5) or during (trials 6–10) water presentation. The filled arrowhead indicates the time of water presentation in each trial. Each black bar denotes an individual licking event. Note that photostimulation in the absence of water

does not lead to drinking after stimulation, even if water is presented a few seconds after the termination of the light stimulation. **b**, Quantification of drinking responses in six animals expressing AAV-flex-ChR2-eYFP in CamKII-positive neurons before (red bar) and during (black bar) water presentation (Mann–Whitney *U*-test,  $P < 0.003$ ). Animals were tested for five trials each, and the total number of licks was averaged across trials. Values are means  $\pm$  s.e.m.



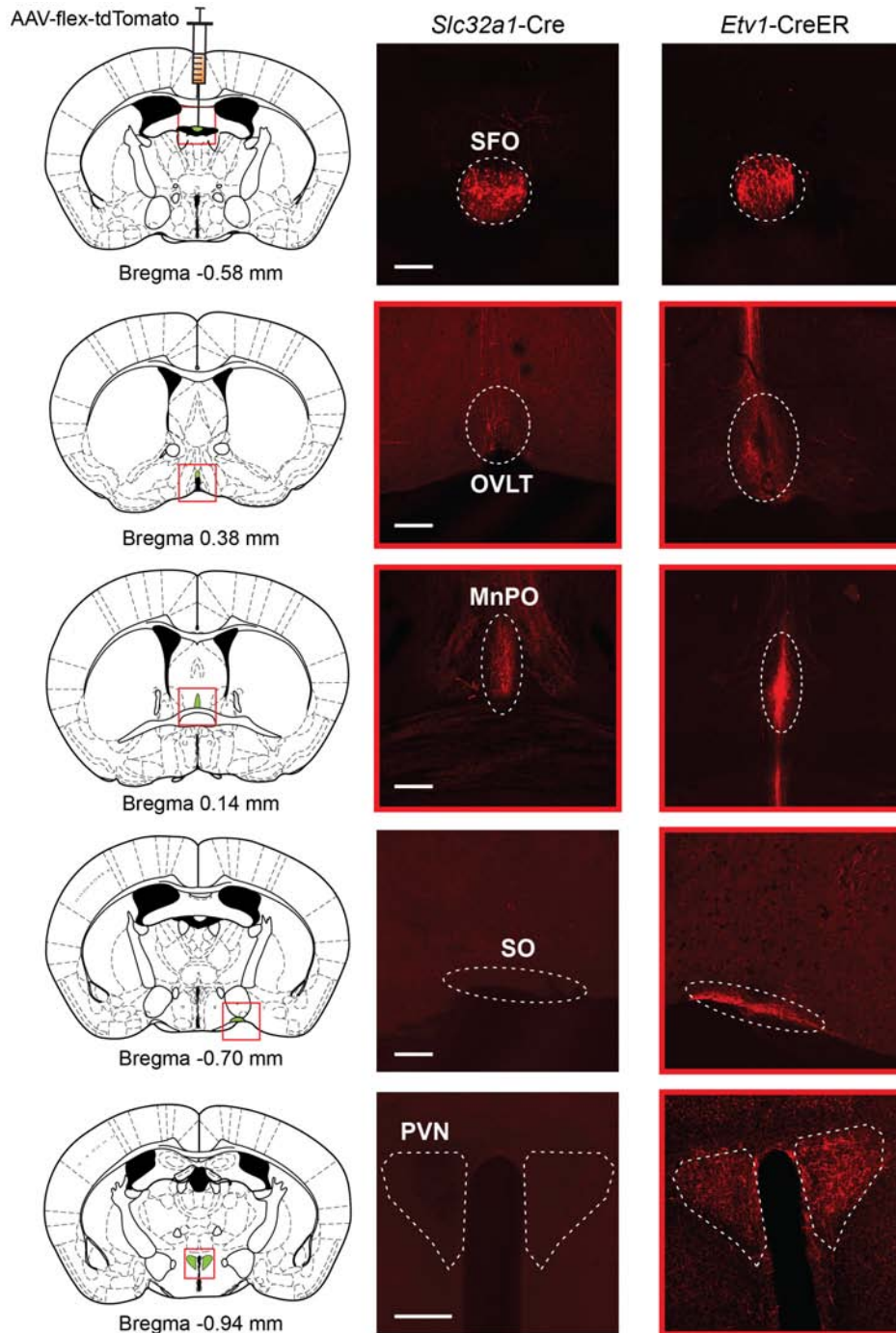
**Extended Data Figure 5 | Three distinct cell populations in the SFO.** Using a combination of data from the Allen Brain Atlas (<http://mouse.brain-map.org>)<sup>31</sup> and a candidate gene approach, we identified three genetically separable, non-overlapping populations in the SFO. One population is defined by the expression of nNOS (red); also overlapping with CamKII- and ETV-1-positive cells (see Fig. 3a, b). A second is a Vgat-expressing population visualized in a

transgenic animal expressing ChR2-eYFP in Vgat-positive neurons (labelled with anti-GFP antibody, green). A third is characterized by the expression of GFAP (white). Shown are double immunohistochemical stainings of nNOS- and Vgat-positive neurons (top panel), nNOS- and GFAP-positive neurons (middle panel), and GFAP- and Vgat-positive neurons (bottom panel). Scale bar, 50  $\mu$ m.



**Extended Data Figure 6 | Angiotensin receptor AT1 is enriched in ETV-1<sup>+</sup> neurons in the SFO.** Quantitative PCR analysis of gene expression in three groups of neurons: ETV-1<sup>+</sup> neurons from the SFO, ETV-1<sup>+</sup> from the cerebral cortex<sup>32</sup>, and Vgat<sup>+</sup> neurons from the SFO. Individual data points were normalized to the levels of GAPDH. Shown are the quantitative PCR results for ETV1, nNOS, Vgat and AT1 in the three different samples; data are presented for each gene as its relative abundance compared with the tissue with the lowest

level of expression (for example nNOS is expressed ten times more abundantly in ETV-1-positive neurons from the cortex than in Vgat neurons from the SFO, and 1,000 times more abundantly in ETV-1-positive neurons from the SFO than the cortex). Note that AT1 is highly enriched in ETV-1<sup>+</sup> SFO neurons. ND, not detected. Values are  $\pm$  s.e.m. ( $n = 3$  technical replicates).



**Extended Data Figure 7 | Neural projections from Vgat- and Etv-1-positive SFO neurons.** *Slc32a1-Cre* (Vgat-cre; left panel) and *Etv1-CreER* (right panel) mice were independently injected with AAV-flex-tdTomato in the SFO, and the axon projections of Vgat-positive and ETV1-positive neurons examined using tdTomato reporter expression (red). Shown are the injection sites (top panels) and representative images of four brain regions receiving

input from the SFO: OVLT, organum vasculosum of the lamina terminalis; MnPO, median preoptic nucleus; SO, supraoptic nucleus; PVN, paraventricular hypothalamic nucleus. Although we cannot preclude additional sites, these four areas exhibited the most prominently labelled projections from the SFO neurons. Scale bars, 200  $\mu\text{m}$ .